Self-Powered Electrostatic Actuation Systems for Manipulating the Movement of both Microfluid and Solid Objects by Using Triboelectric Nanogenerator

Li Zheng, Yali Wu, Xiangyu Chen, Aifang Yu, Liang Xu, Yongsheng Liu, Hexing Li, and Zhong Lin Wang**

By integrating a triboelectric nanogenerator (TENG) and an electrostatic actuation system (EAS), two kinds of self-powered EAS are designed for manipulating the movement of both microfluid and tiny solid objects. The mechanical triggering of the TENG can generate an extremely high electrostatic field inside EAS and thus the tiny object (liquid or solid) in the EAS can be actuated by the Coulomb force. Accordingly, the tribomotion of TENG can be used as both the driving power and control signal for the EAS. The TENG device with a contact surface of 70 cm^2 can drive a water droplet to move across a gap of 2 cm. Meanwhile, the confluence of two droplets with the same charge polarity and different components can also be induced and controlled by this self-powered EAS. In addition, based on the same working principle, this EAS also demonstrates its capability for manipulating solid object (e.g., a tiny steel pellet). By sliding the Kapton film along a segmented annular electrode, the tiny pellet can well follow the rotated motion of the Kapton film. The demonstrated concept of this self-powered EAS has excellent applicability for various micro/miniature actuation devices, electromechanical systems, human–machine interaction, etc.

1. Introduction

The technologies of self-powered nanosystems are receiving intensive attention due to their huge applications in portable/wearable electronics, active sensor, and human–machine interfacing.[1–3] The conceiving of this concept is due to the dramatic development of all kinds of renewable energy harvesting technologies, among which triboelectric nanogenerator (TENG) that can directly convert various mechanical motions into electrical energy is proved to be an ideal technique to serve as the core element of self-powered systems.[4–8] The advantages of TENGs lies in its simple fabrication processes, low cost, environmental friendliness, and extensive availability of the target resource, which are highly preferred for a variety of multifunctional nanosystems.[9,10] Not only working as a power generator to supply some microelectronic devices, the TENG can also generate spontaneously high electrostatic field from the contact or tribomotion, which allows TENG to function as a high voltage source to control some smart electromechanical systems and to realize various interesting applications in the field of optical devices and wearable electronics.[11,12] As for the TENG-based electromechanical systems, a human or mechanical motion can play dual functions as both the driving power and the control signal. Hence, TENG can be utilized as a bridge for human–machine interactions, where both the additional power source and the sophisticated control circuits can be spared, thus the proposed self-powered nanosystems can be achieved. Accordingly, all these progresses inspired us to keep developing some novel and practical applications for TENG technology in the field of the electromechanical systems, in order to further popularize this excellent human/environment-interactive capability of TENG.

In comparison with electromagnetic or piezoelectric actuation, electrostatic actuation based on Coulomb force has been considered as an ideal strategy for driving or manipulating micro/nanoobjects.[13] Advantages of the electrostatic actuator as well as the related electromechanical system include effectiveness, low-power, fast-response speed, and so on.[14,15] Especially for the small electrode gap case, the reduction of the size will further enhance its efficiency due to basic law of the Coulomb force. Accordingly, a series of progresses have been made for the application of this actuation technology in the field of

Dr. L. Zheng, Y. Wu, Dr. X. Chen, Dr. Y. S. Liu, Prof. H. Li
School of Mathematics and Physics
Shanghai Key Laboratory of Materials Protection and Advanced Materials in Electric Power
Shanghai University of Electric Power
Shanghai 200090, China
E-mail: chenxiangyu@binn.cas.cn

Dr. L. Zheng, Dr. X. Chen, Dr. A. Yu, Dr. L. Xu, Prof. Z. L. Wang
Beijing Institute of Nanoenergy and Nanosystems
Chinese Academy of Sciences
National Center for Nanoscience and Technology (NCNST)
Beijing 100083, China
E-mail: zlwang@gatech.edu

Prof. Z. L. Wang
School of Material Science and Engineering
Georgia Institute of Technology
Atlanta, GA 30332-0245, USA

DOI: 10.1002/adfm.201606408

high frequency switches, oscillators, motors, and microfluidic device.[16,17] Coulomb force is the direct product of the electrostatic field, while the TENG can generate an extremely strong electrostatic field even with a very small volume of device. On the other hand, in previous study related to the self-powered actuation system,[11,12] the leakage of the tribo-induced charges through the dielectric elastomer always jeopardize the performance of the conjunction system, which is the most serious problem for its practical application.[11] In comparison with the soft elastomer actuators, the charge leakage through the electrostatic actuator is infinite small, which is more ideal for maintaining the tribo-induced electrostatic field. Hence, TENG can be smoothly integrated with the electrostatic actuation system to realize a self-powered and motion-tunable actuation system, where all of the advantages of the electrostatic actuator, such as effectiveness and fast response, can be carried forward by the good compatibility of the TENG.

In this study, we have proposed a concept of self-powered manipulator and actuator by coupling an electrostatic actuator and a TENG device. Based on the high electrostatic field generated from TENG devices, we can directly manipulate the motion of both the microfluid and solid pellets through the Coulomb force. Accordingly, two kinds of self-powered electrostatic actuation systems (EAS) for both the microfluid and solid pellets is established and the tiny liquid/solid objects, which cannot be easily activated by the common mechanical tools, can possibly be accurately manipulated only by simple manual operations imposed on TENG devices. Here, the contact–separation or sliding motions can serve as both driving power and regulating signal, and thus no power source or sophisticated control circuits are needed for this system. Given a collection of advantages, our results show great potential applications of TENG as an enabling technology in the field of the electromechanical system, microsolid/liquid manipulator, human-robotic interaction, and so on.

2. Results and Discussion

2.1. Self-Powered EAS for Manipulating Microfluid

The structure of the integrated EAS based on single-electrode TENG to manipulate the motion of microfluid is shown in **Figure 1**a. The single-electrode TENGs are employed as the core element of the system,[18] whereas the output voltage is generated by contact electrification process happened between Kapton film and Al foil. Two strip electrodes made of indium tin oxide (ITO) are placed underneath a superhydrophobic nanostructured fluorinated ethylene propylene (FEP) film to form a simple EAS structure, where one electrode of EAS is grounded and the other electrode is connected to the TENG. A distilled water droplet is dropped in the gap between two strip electrodes, as shown in Figure 1a. It is worth noting that the charge on the water drop without any special treatment is usually positive due to the contact electrification between water drop and air.[19–21] The contact–separation motion of the Kapton film can trigger the establishment of high electrostatic field between two strip electrodes. Meanwhile, the mechanical motion can serve as both the power supplier and the controlling signal. Accordingly, the Coulomb force generated by this high electrostatic field can move the water droplet from one electrode to the other. This is the basic operation mechanism of this EAS system. Furthermore, the inductively coupled plasma (ICP) treatment is applied on the surface

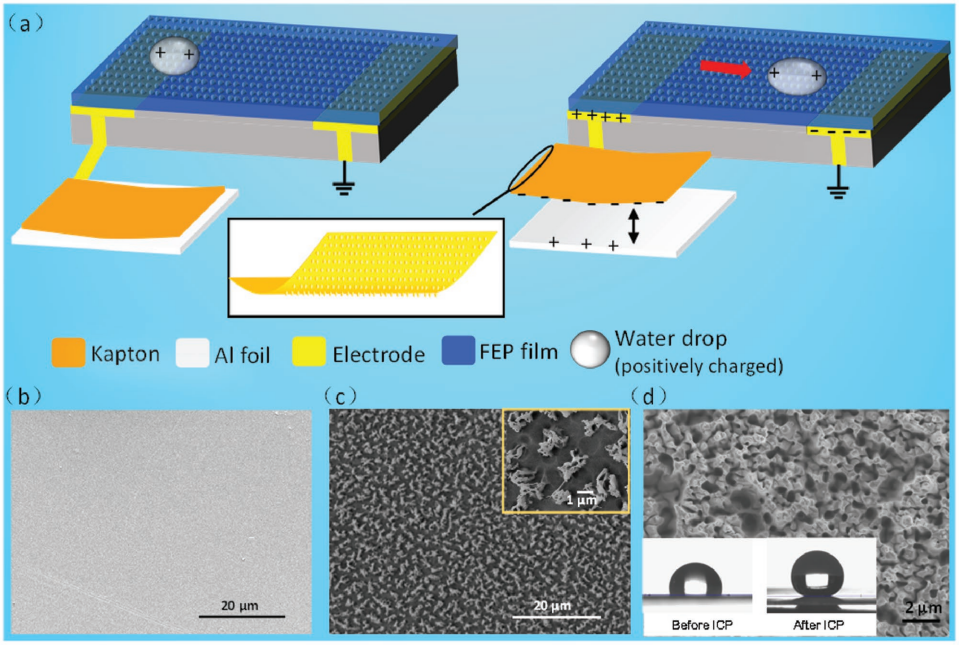

Figure 1. Schematic illustration of the self-powered EAS for manipulating microfluid. a) Structure design of the SMM based on a single electrode TENG for driving a water drop. b) SEM image of the Kapton film before ICP treatment. c) SEM image of the Kapton film after ICP treatment. d) SEM image of the FEP film after ICP treatment. Insets: The contact angle of FEP film before and after ICP treatment.

of Kapton film in order to enhance the electrification performance.[11,12] Hence, the Kapton film is coved by a series of nanopatterned structure and the corresponding scanning electron microscopy (SEM) images can be found in Figure 1b (before ICP treatment) and Figure 1c (after ICP treatment). The improved contact surface of TENG can be obtained by this kind of surface modification process. The electrical output performance of the single-electrode TENG is systematically studied as shown in Figure S1a,b in the Supporting Information, where the output open-circuit voltage (V_{oc}) is about 1800 V and the transferred short-circuit charge (Q_{sc}) is 250 nC. It is important to note that no electrical damage has been observed in the EAS system under such a high voltage, since FEP films are very good insulators. Meanwhile, the output current from TENG as well as the transferred charges are all quite small. The established electrostatic field will vanish quickly if some leakage phenomenon happens. For the electrical measurement of the TENG, the effective contacting area of single electrode TENG is about 70 cm^2 (7 cm × 10 cm), while the applied pressure on the TNEG is about 800 Pa. The motion velocity for the measurement is controlled to be 1 m s^{-1}. The short circuit current for the TENG is about 3.9 μA, as can be seen in Figure S1c in the Supporting Information. As for the measurements of the high output voltage from TENG, we modified an electrostatic voltmeter (Monroe ME-297) and use its dynamic module to catch the performance of the V_{oc}. The Monroe ME-297 voltmeter is usually used for checking the surface potential of the electrified materials and it has a very high internal resistance, which can help to maintain the tribo-induced charges on TENG. The distribution of the electric field is also measured by directly using the ME-297 voltmeter, as can be seen in Figure S1d in the Supporting Information. The probe of the voltmeter is placed very close to the strip electrode (less than 1 mm), in order to avoid the electrostatic interference. The probe can be moved in plane region and thus the electric field distribution near the electrode can be detected. The highest potential can be obtained right on the electrode and the potential value gradually decreases when the probe moves away from the electrode. The superhydrophobic porous structures on FEP surface are also conducted using ICP etching, where the SEM image of the FEP surface is shown in Figure 1d. The mean diameter of the holes determined from SEM images is around 300 nm. Because the porous nanostructures contain trapped air, it will reduce the actual contact area between the surface and the water droplet, making the surface superhydrophobic. The inset photos in Figure 1d give the change of contact angle before (95°) and after fabricating nanostructures (154°). The superhydrophobic surface will ensure the water droplet to move smoothly on the surface of FEP, which effectively enhance the performance of the actuation.

The detailed working mechanism of this EAS is illustrated step by step in **Figure 2**a. The manipulation of the water droplet is based on two triboelectrification processes, one happened on Kapton–Aluminum interface and the other happened on water–FEP interface. During the contact motion between Kapton film and Al foil, positive and negative charges are electrostatically induced on the surface of Al foil and Kapton film, respectively. After that, the separation motion between two objects leads to a high voltage output between Al foil and the ground.[11,12] Then, this output voltage is applied on the EAS connected to Al foil and the motion of the water droplet will be activated. The excessive positive charges on the water droplet are due to the electrification with the air. When the electrostatic field between two electrodes is established, a Coulomb force will be applied on the positively charged water to move it away from the positively charged electrode and to move close to the negatively charged electrode. The strength of this Coulomb force is determined by the generated tribo charges from TENG and the gap distance between two electrodes. During the sliding motion, the triboelectrification process between the water droplet and the FEP film also happens, which leaves negative charges on the FEP surface and induces more positive charges on the water droplet. It is important to note that the triboelectrification process between the water droplet and the FEP film also induces a Coulomb force, as illustrated in Figure 2a. When the top plate with Kapton film moves back and contacts Al foil again, the positive charges on Al foil are neutralized and the established electric field vanishes. In this case, the Coulomb force existed between the water droplet and the FEP film leads to the original position. On the other hand, even though the charge leakage through the EAS is negligible, the slight charge leakage can happen on the Al foil of TENG during the operation, which can be attributed to the neutralization process caused by the free ions in the ambient air.[22] This charge leakage process results in an opposite electric field established between two strip electrodes (V', $V' \ll V$). As can be seen in the output performance of the TENG in Figure S1a in the Supporting Information, the output voltage from TENG changes to −300 V, when the top plate (Kapton) moves back to the contact position. This opposite electric field will further facilitate the return of the water droplet. However, if the gap between two electrodes is too large, the water droplet cannot move back. As shown in Figure 2b, the positive charges on the water droplet cannot be increased infinitely, which means the charged zone on the FEP surface has a maximum width due to the charge saturation of the water droplet.

In order to confirm the existence of this charged zone and the interval (see Figure 2b), an additional experiment is performed to study the generated electric field between FEP film and water droplet, which can be seen in Figure S2a,b in the Supporting Information. In this experiment, the strip electrodes are removed from the system and we can only study the interaction between water droplet and FEP film. First, a water droplet (40 μL) is dropped onto the FEP film (zero position) and then it straightly slides across the FEP film in one direction. Along the motion trace of the water droplet, the surface potentials on the FEP film before and after the contact with water droplet are measured by using an electrostatic voltmeter. The results of the obtained surface potential are shown in Figure S2a in the Supporting Information. After the water droplet slides across the FEP film, the surface potential on the FEP film is decreased significantly, which confirmed that the FEP film will be negatively charged due to the contact electrification with water droplet. Meanwhile, the potential differences on the FEP film before and after contact with water droplet are summarized, as can be seen in Figure S2b in the Supporting Information. For the first point, the potential difference can reach 400 V, while for the second point (0.5 cm) the potential

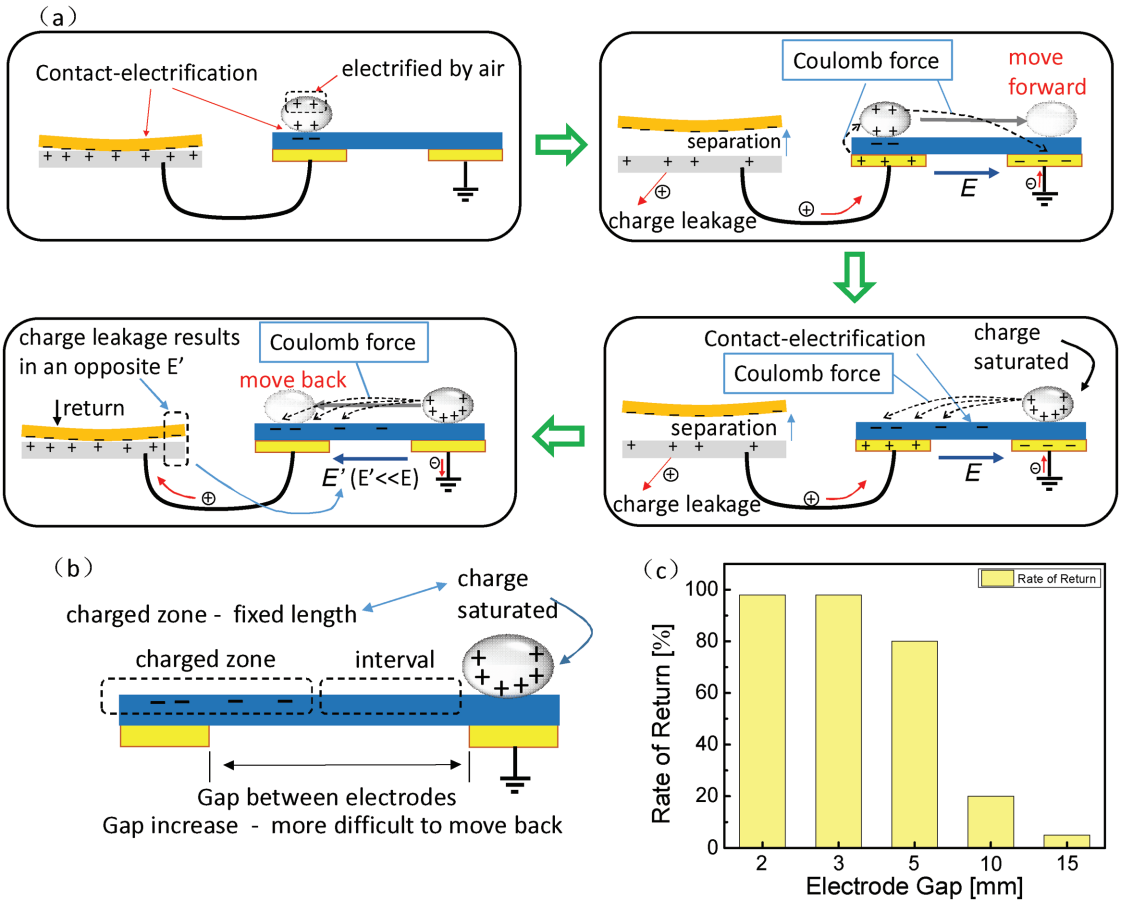

Figure 2. a) The working principle of the EAS, where the Coulomb force induced by contact-electrification can serve as the driving force to control the motion of small water droplets. b) The detailed illustration of the contact-electrification process between water droplet and FEP film, which can induce a coulomb force to move back the droplet. c) The return rate of the water droplet with the increase of the gap, where return rate is defined as backward distance over forward distance.

difference is only 200 V. After a sliding distance of 2.5 cm, the potential difference is close to zero, which is due to the charge saturation of the water droplet. This experiment confirmed the existence of the charged zone. Accordingly, if the sliding distance is quite short (<1 cm), the water droplet can experience a drag force due to the negative charges on FEP film. However, if we keep increase the sliding distance, the influences of the negative charges on FEP film will be decreased significantly. We further studied the motion characteristics of the water droplet with different gap distances (see Figure 2c), where the rate of the return is defined as the backward distance over forward distance. Here, the results shown in Figure 2c are the average results after repeating the experiments more than 10 times. Accordingly, with the increase of the gap length, the interval between the water droplet and charged zone on the FEP also increases and thus the return of the water droplet becomes more and more difficult. The detailed demonstration of the motion of the water droplet can be seen in Movies S1 and S2 in the Supporting Information. On the other hand, it is necessary to check the minimum voltage for moving microfluid by using a power supply, in order to confirm the high output voltage from TENG. Hence, we prepared another video material (Movie S5) in the Supporting Information. Under the actuation of the power source, the water droplet starts to move until the applied voltage reaches 3500 V, while the TENG can easily move the droplet by simple separation motion. This experiment confirmed the superiority of the TENG for driving EAS. Meanwhile, it also suggests that the real output voltage from TENG is much higher than the value we obtained from electrical measurement. The reason for this can be attributed to the leakage phenomenon happened through the voltmeter. For better measurements, we may need some specially designed high resistor to fully isolate the tribo-induced charges, which can achieve very precise measurement of the voltage drop.

For the operation measurement of the prepared self-powered EAS, the top plate adhered by Kapton film is the movable object while the bottom plate adhered by Al foil is fixed, and a linear motor is applied to guide the vertical separation motion of the top plate. The motion of the linear motor is a symmetric acceleration–deceleration mode, while the acceleration rate is controlled to be ±20 m s^{-2}. First, the driven distance of the water droplet with different volume is measured, as displayed in **Figure 3**a. In this measurement, the initial distance of the water droplet is defined as the distance from the edge of the electrode to the same edge of the water droplet (see the inset of Figure 3a), which is fixed to be zero for measurements in

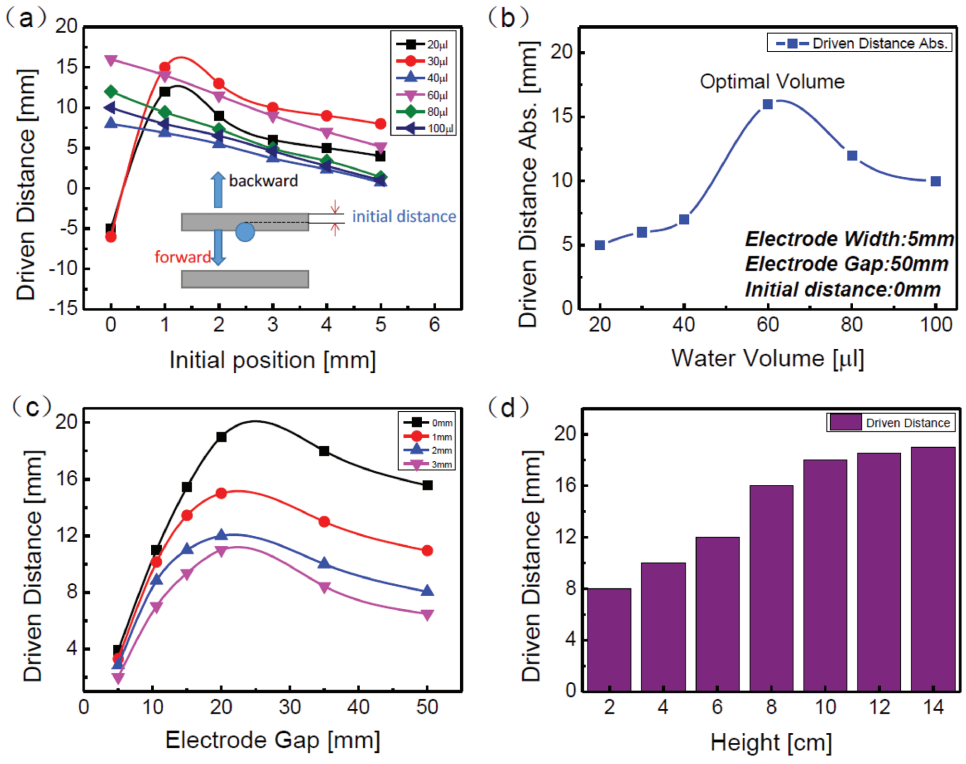

Figure 3. The detailed operation performance of the EAS. a) The driven distance with different initial positions. b) The influence of water droplet volume to the driven distance. c) The driven distance with different electrodes' gap length. d) The driven distance with different separation heights of TENG.

Figure 3a, and the driven distance is the position change of the water droplet. The gap between two electrodes is 50 mm, while the single-electrode TENG is connected with the electrode near the droplet. Accordingly, under the activation of the TENG, even though the charges on two electrodes (positive and negative) can both apply Coulomb force on the water droplet, while the TENG-connected electrode provides the dominating driving force. Hence, for the water droplet larger than 40 μL, the increase of the initial distance leads to the decrease of the driven distance, since the Coulomb force is inversely proportional to the distance between two charged objects. Meanwhile, it is interesting to find that the motion distance is in the backward direction for the case of water droplet with volume of 20 and 30 μL. In these two cases, the radius of the droplet is smaller than the half-width of the electrode. Hence, when the electrode is positively charged by the TENG, the droplet will move backward (away from the grounded electrode) in order to efficiently get away from the electrode. This experiment proves that the initial position of the droplet is the key factor for determining the motion direction, since the pulling force from the grounded electrode is very small in this case. The driven distances of the water droplet with different volumes are summarized in Figure 3b, where the optimized volume for this condition is 60 μL and the maximum driving distance is 16 mm. As for the water droplet with small volume cannot move more distance than large one, it is due to many effects. With the decrease of the volume, the weight of the droplet is decreased and accordingly the required driving force for moving the droplet is also decreased. However, the decrease of the surface area also results in the decrease of the carried charge amount on the droplet. Hence, the generated electrostatic force between droplet and the electrode is decreased correspondingly. The gap distance is another important factor for this self-powered EAS. The driven distance with different gap lengths is explored in Figure 3c, where four different initial positions are selected for the experiment as references. Here, by decreasing the gap distance, the pulling force from the grounded electrode increases correspondingly and thus the driven distance of the droplet also increases. With the initial position of zero, the maximum driven distance of 19 mm can be achieved under a gap distance of 20 mm. Hence, the gap distance of 20 mm is the optimized value for this set of EAS. For analyzing the performance of this self-powered EAS under the control of mechanical motion, we prepared several experiments to study the handling characteristics of this EAS system. The dependence of driven distance with separation height of TENG is shown in Figure 3d (the velocity is 10 cm s^{-1} and four tribosurfaces are chosen). With the increase of the separation height, the driven distance increases gradually and the driven distance stops increasing until the separation distance increases up to 10 cm. On the other hand, the different motion velocities can only slightly influence the driven distance (see Figure S1e in the Supporting Information). For the velocity larger than 3 cm s^{-1}, the activated motion of the droplet is almost the same, since the relaxation of tribocharges need at least tens of seconds.

To further explore the practicability of this self-powered EAS technology, we present another structure of EAS to simultaneously control the confluence motion of two different droplets (with the same charge polarity). The structure of as-fabricated EAS as well as the basic operation process are both shown in

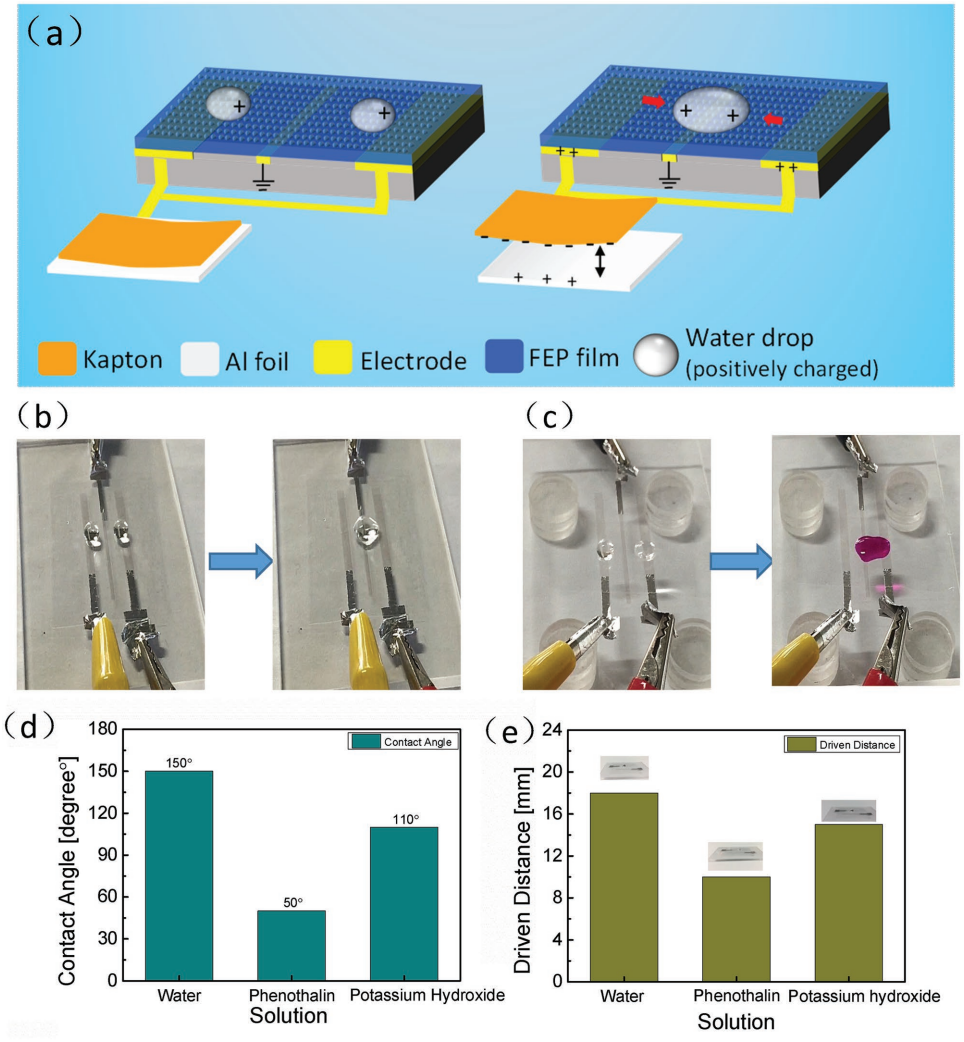

Figure 4. Application of the EAS for controlling the confluence of droplets. a) The design of the manipulator and the working mechanism. b) The photographs of two water droplets before and after the confluence. c) The photographs of two kinds of phenothalin and potassium hydroxide droplets before and after the confluence. d) The contact angles of FEP film for three different solutions. e) The driven distance for three different solutions (distilled water, phenothalin, and potassium hydroxide, respectively). The volume of all three solutions is 40 µL.

Figure 4a. Two side strip electrodes are both connected to the Al foil of the TENG and one middle strip electrode is grounded (see Figure 4a). During the confluence of two positively charged droplets, the positive charges on both droplets result in a coulomb force to push them away from each other. While two droplets approach each other, this pushing force gets stronger and finally two droplets may bounce off each other.[23,24] It is important to note that for the liquid droplets (water or other liquids), the contact electrification with open air or with micropipettor can usually induce positive charges on the droplets.[25] Hence, it is necessary to design some EAS for controlling the confluence of two positively (or two negatively) charged droplets. In our TENG-based EAS, with the motion of the Kapton film, the two electrodes connected with Al foil are positively charged and the generated Coulomb force drives the two droplets to move toward each other. Meanwhile, the negative charges on the grounded electrode in the middle can offer a pulling force for both of the two droplets, which can help them to overcome the bouncing force between them. The detailed demonstration of the confluence of two different droplets can be seen in Figure 4b and the video demonstration can be found in Movie S3 (Supporting Information), where two water droplets converge at the middle grounded electrode under the driving of the TENG. The water droplets can also be replaced by chemical solutions. As can be seen in Figure 4c, the phenothalin droplet and potassium hydroxide droplet are dropped on the two outer electrodes, respectively, while the confluence of two droplets can be induced on the middle grounded electrode. Meanwhile, the redox reaction happens during the confluence of two droplets, which changes the color of the converged solution from transparent to red, as revealed in Figure 4c and Movie S3 in the Supporting Information. The different solution may result in different contact angles between FEP film and the droplets, as listed in Figure 4d. The contact angle of potassium hydroxide droplet is 105°, while that of phenothalin is reduced to be 50°. The captured photograph of the contact angle can

be seen in Figure S3a,b in the Supporting Information. The detailed relationship between contact angle and the sliding motion of the droplet has been intensively studied by the other researchers.[26,27] Generally speaking, the sliding motion of water droplets becomes easier with the increase of contact angles in the highly hydrophobic region. The interaction energy between water and substrate is proportional to the true contact area and thus the increase of the contact angle decreases this interaction energy. As shown in Figure 4e, under the same driving conditions, the phenothalin droplet has the shortest driven distance and the distilled water droplet with the highest contact angle on FEP film surface has the longest driven distance. This experiment well demonstrated the application of this self-powered EAS in the field of chemical and biological technology, where the EAS can be integrated with microscope to manipulate and observe the motion of different solutions. It is also necessary to note that the change of the driven distance can be decided by many factors, including contact angle, carried charge amount, and the electrification characteristics referring to FEP film. Hence, the detailed explanation related to the change of the driven distance for different solution still requires further study. On the other hand, some fluid channel can be applied to the EAS to precisely regulate the motion of the droplet, as shown in Figure S4 in the Supporting Information. Here, the fluid channel is made of polydimethysiloxane (PDMS) film. However, we found that even though the motion direction of droplet can be regulated very well, the driven distance is increased significantly, which may be due to the change of the contact condition between droplet and FEP film. In order to better improve the motion of the droplet in the channel, a better fabrication method is necessary. Based on all these experiments, we confirm that the motion of the liquid droplet with different components can be driven by this unique operation method of TENG-based EAS, while both the motion distance and the motion direction of the droplet can be regulated by the contact–separation motion of the TENG.

2.2. Self-Powered EAS for Manipulating Solid Object

The concept of this self-powered EAS provides a promising application of TENG as a motion-tunable actuator to drive and to control various micro-electromechanical systems. Not only liquid microfluid, but also some tiny solid objects need to be manipulated. As can be seen in **Figure 5**a, in order demonstrate the capability of this self-powered ESA for manipulating solid objects, an actuation system based on the similar single-electrode TENG is established for driving a tiny pellet. In this system, a tiny pellet (steel, 8 mg) is hanged by a string made of carbon fiber and is located near the strip electrode.

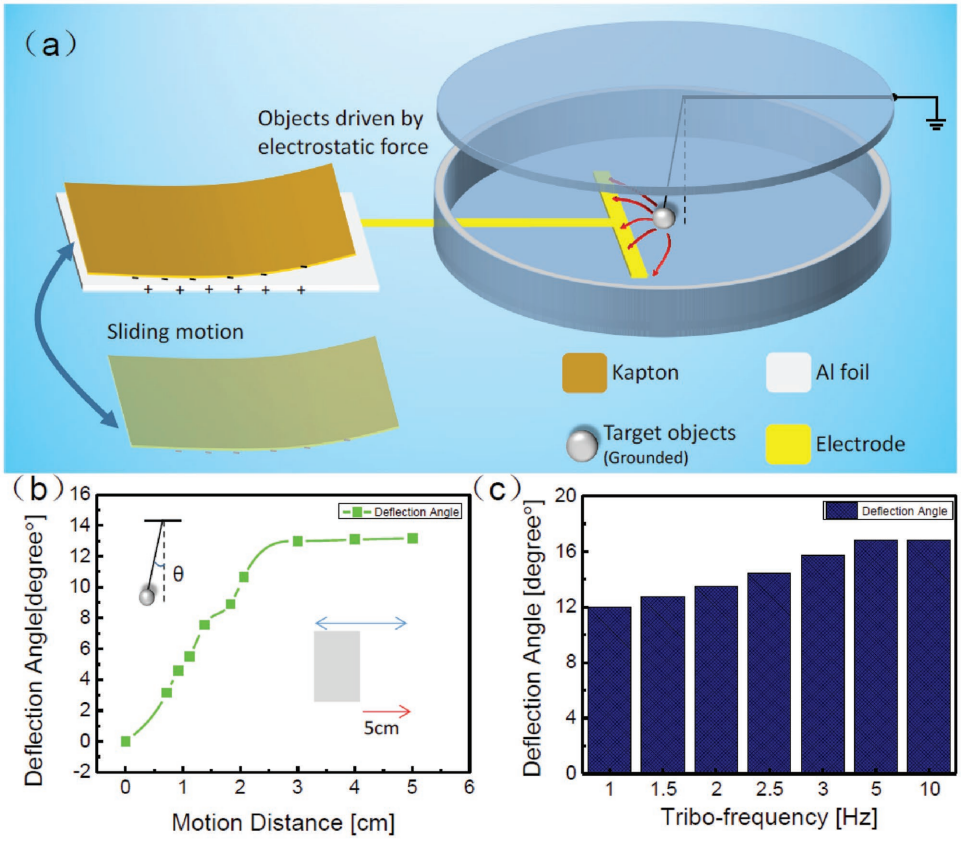

Figure 5. The self-powered EAS for driving tiny solid object. a) The structure design of the EAS system, where a similar single-electrode TENG is applied to generate Coulumb force to control the solid pellet. b) The deflection angle of the pellet under the driving of the TENG, where different separation distances are applied to the contact-TENG device. c) The deflection angle of the pellet with different motion speeds of the Kapton film, where the motion distance is fixed to be 5 cm.

The steel pellet is grounded with the carbon fiber. The working mechanism of this EAS is similar to the previous system for microfluid, whereas the sliding motion instead of contact–separation motion is applied to TENG. The structure of the TENG used here can still be considered as working in single-electrode mode. However, for the solid pellet's case, the pellet is grounded by the carbon fiber (no charges on it before the actuation) and the negative charges induced by the TENG on the pellet originate from the ground. On the other hand, for the water droplet's case, the charges on the water droplet are generated by the contact electrification between water droplet and other materials. This is the most significant difference between two kinds of systems. The detailed mechanism is illustrated in Figure S5 in the Supporting Information. The sliding motion can provide some continuous actuation to the pellet, which will be introduced later. When the Kapton film is separated from the Al foil, a strong electric field is established between strip electrode and the steel pellet (grounded) due to the positive charges remained on the Al foil. Attracted by the Coulomb force, the pellet shows a deflection angle, which can reveal the intensity of the electrostatic field generated by TENG. As displayed in Figure 5b, the deflection angle of the pellet (under steady states) increases with the increase of the motion distance of the Kapton film, which indicates good operating characteristics of this TENG-based EAS. The detailed value of this deflection angle can be captured by using high-speed camera and the maximum angle is about 13.5° at the sliding distance around 4 cm, as shown in Figure 5b. Unlike the EAS for microfluid, the force situation of the pellet in this EAS is much more complicated. Therefore, we offered a detailed analysis of the forces applied on the pellet, as shown in Figure S6 in the Supporting Information. Without the actuation of the TENG, the gravity (G) and the pulling force (F_p) from carbon fiber is in balance (see Figure S6 in the Supporting Information). When the electrostatic field is applied by TENG, the Coulomb force (F_e) from the strip electrode will be applied on the pellet (Figure S6, Supporting Information). Accordingly, a deflection angle (θ) is induced between deflected carbon fiber and the vertical direction. Both angle θ and angle α (16.7°) can be calculated based on the photograph captured by the camera. The force balance of the ball needs to satisfy the relationship: $F_p \cdot \cos\theta = F_e \cdot \sin\alpha + G$ and $F_p \cdot \sin\theta = F_e \cdot \cos\alpha$. Hence, the Coulomb force applied on the pellet is 23 μN (θ = 13.5°). The increase of the deflection angle is decided not only by the Coulomb force but also by the force angle α, and thus α = 16.7° is the highest value we can get under steady state. On the other hand, the deflection angle of pellet under the reciprocating motion is different from the steady state, while different motion frequency can also influence the deflection angle. With the increase of the motion frequency (see Figure 5c), the deflection angle of the pellet is increased correspondingly, and this phenomenon is possibly due to the relaxation of the tribocharges and the resonance behavior of the pellet system. The optimized frequency for activate this EAS is about 10 Hz, as shown in Figure 5c.

In order to illustrate the potential applications of this EAS as the manipulator for the solid objects, we demonstrated a further designed EAS with segmented annular electrodes to lead the rotated motion of the pellet. The structure design of this EAS in shown in **Figure 6**a. An annular electrode with four segments is selected as the electrode of TENG, while the Kapton film slides over on the surface of each segment successively. Correspondingly, the output terminal of the EAS is also an annular electrode with four segments and each segments is connected with one of the output electrodes of the TENG. The steel pellet (8 mg) is grounded and hanged in the center of the annular electrodes through a carbon fiber. The inner and outer diameter of the annular electrode in the EAS near the pellet is 6 and 10 mm, respectively, while the annular electrode in the sliding TENG has an inner and outer diameter of 5 and 20 cm, respectively. For the electrical measurement of the TENG, the output voltage can reach 2300 V, when the effective contacting area of each segment of the annular electrodes is about ≈80 cm^2 and the applied pressure on the TNEG is about 800 Pa. The results can be seen in Figure S7 in the Supporting Information. In this EAS, four single-electrode TENGs are integrated together, where each segmented electrode in EAS applies a Coulomb force on the grounded steel pellet. Accordingly, the motion of the pellet is decided by the integrated force of four electrodes. Theoretically, in the ideal case without considering the deviation of the overlapped area, the negative charges on the Kapton (Q_k) surface are equal to the total positive charges (Q_A) on four Al foil ($Q_k = 4Q_A$) after the Kapton film moving around a full cycle on four annular Al foils. In this case, if the Kapton film totally overlapped one segmented electrode, the effective negative charge amount ($Q_k - Q_A = 3Q_A$) on that electrode should be three times larger than that on each segmented electrode (the charge neutralization between Kapton film and the contacted Al foil is included in this calculation). Hence, the pellet is pulled toward the electrode overlapped by the Kapton film due to the stronger Coulomb force. With the Kapton film sliding along the segmented annular electrode one by one, the steel pellet is rotated simultaneously. The demonstration of this rotating EAS can be seen in Movie S4 in the Supporting Information, where both clockwise and anticlockwise rotations of the pellet have been induced. As shown in Figure 6b, the deflection angle of the pellet is decided by the area of the Kapton film, which confirms the dominant contribution of the TENG. On the other hand, the established deflection angle of the pellet in response to different rotation speed of Kapton film can also be measured by high speed camera, as illustrated in Figure 6c. It is interesting to find out that the deflection angle of the pellet tends to saturate if the rotating speed of the Kapton film is too high and the optimized motion speed is decided to be 1.5 r s^{-1}. In a high speed case, before the pellet can fully react to the Coulomb force, the Kapton film has already moved to the next electrodes. Thus, the deflection angle of the pellet is gradually decreased due to the excessive increase of the sliding speed of the Kapton film, as can be seen in Figure 6b. Since it is only a prototype, we believe that the performance and the application perspective of this EAS can be further improved by developing more delicate fabrication techniques.

3. Conclusion

In summary, by directly utilizing the strong electrostatic field generated from a single-electrode TENG, we have

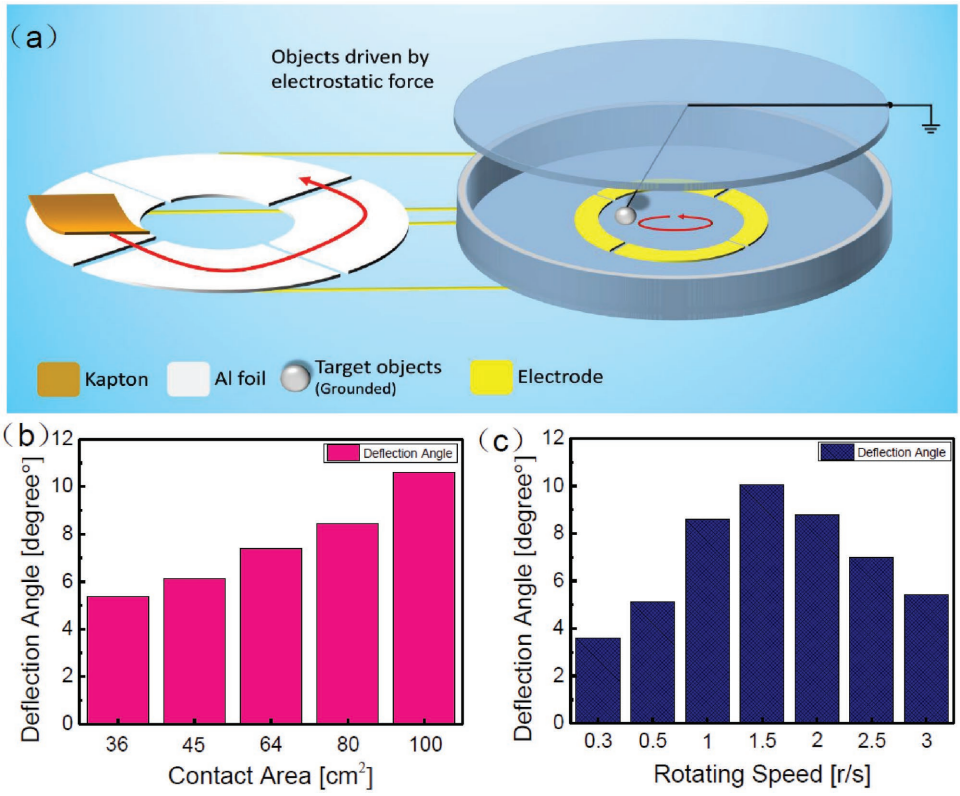

Figure 6. The further demonstration of the self-powered EAS for leading rotated motion of the pellet. a) The structure design of the driving system, where segmented annular electrodes are employed for TENG. b) The deflection angle of the pellet under the driving of the TENG, where different contact areas are selected for TENG. c) The deflection angle of the pellet with different sliding motion speeds inside the TENG device.

demonstrated a novel self-powered EAS to provide controllable actuation on both microfluid and tiny pellet. The separation motion of the TENG with a contact surface of 70 cm^2 can drive a distilled water droplet to move across a gap of 20 mm. The separation distance of TENG is for manipulating the motion of the droplet, while the system can stably function with different contact–separation velocities (2–10 cm s^{-1}). The confluence of two droplets with different components can also be realized by using this EAS under the driving of the contact electrification, indicating the potential application of this EAS as an easily fabricated experimental tool to delicately control the cell motion in some biological and chemical researches. On the other hand, a similar self-powered EAS has also been applied to manipulate the slide and rotation of a tiny steel pellet, further demonstrating the universal applicability of this self-powered EAS. The concept of this TENG-based EAS has extensive applicability due to its high efficiency and fast response characteristics. A wide variety of potential applications can be demonstrated based on this conjunct system, including ink-jet printing, electrospray ionization for mass spectrometry, the microreactors in microfluidic devices, scrubbers for removing particulates, drug delivery in microscale, and so on. Meanwhile, considering the self-powered capability and the motion-controllable characteristics of TENG, this TENG-based EAS could potentially serve as the bridge for human–machine interactions.

4. Experimental Section

Design and Measurement of Single-Electrode TENG: The single-electrode TENG designed for this experiment had two plates (a fixed one and a moveable one) to serve as motion objects. Here, the supporting substrates were employed on each plate to ensure the close contact during its motion. For the fixed plate, an Al foil with rectangular shape (10 cm × 10 cm) was attached on its top surface, where the foil could functionalize as both tribosurface and the output electrode. The other tribosurface was the surface of a Kapton adhesive tape (thickness ≈50 µm, 7 cm × 10 cm), which was adhered on the surface of the moveable plate. The ICP reactive-ion etching process was performed on the surface of Kapton tape, in order to achieve nanopatterned structures. The detailed parameters for the ICP treatment could be seen in the reference paper.[11] For the electrical measurement, the single-electrode TENG was driven periodically by a numerical controllable linear motor, where the two plates were kept in parallel with each other and their inner surfaces was in intimate contact. The output performance, including output current/voltage, potential distribution, and so on, was measured by an oscilloscope, Stanford Research Systems and a Monroe ME-297 electrometer. Tektronix DPO3034 oscilloscope and Kethiely 4200 were used to detect the transferred charges.

Fabrication of EAS: The strip electrodes for manipulating microfluid were made of ITO for keeping the transparency of the devices and the electrodes were deposited by magnetron sputtering. The FEP film with designed nanostructured surface was attached on top of strip electrodes and the water droplet could move smoothly on the surface of the FEP film. The nanostructures on the FEP surface were also fabricated by using the ICP reactive ion etching. In the etching process, a Cu film with a thickness of around 25 nm as the mask was deposited on the FEP surface. A mixed gas (Ar, O_2, and CF_4) was applied in the ICP chamber

(corresponding flow rates were 15.0, 10.0, and 30.0 sccm, respectively). The nanostructure was etched under a power source of 200 W to generate a large density of plasma. For the EAS to drive solid pellet, the electrodes were made of Al foil, while the tiny pellet was made of steel with a weight of 8 mg. The highly conductive carbon fibers were employed to hang the pellet and were connected to the ground. Both the sliding motion and the rotation motion of the Kapton film were guided by digital motors, where the sliding distance and the motion speeds could be controlled by the monitoring circuits. The deflection angle of the pellet was recorded by a fixed high-speed camera (PHOTRON, AX200). All the electrodes as well as the pellet were all sealed in a box to avoid the environmental influences from surroundings.

Supporting Information

Supporting Information is available from the Wiley Online Library or from the author.

Acknowledgements

This work was supported by the National Key R&D Project from Ministry of Science and Technology (2016YFA0202704), the "thousands talents" program for pioneer researcher and his innovation team, China and National Natural Science Foundation of China (Grant Nos. 2016YFA0202704, 61405131, 51432005, 11374204, 5151101243, 51561145021), Shanghai Pujiang Program (No. 16PJ1403500), "Shu Guang" project of Shanghai Municipal Education Commission (No. 13SG52), Science and Technology Commission of Shanghai Municipality (Nos. 14DZ2261000, 14520501000), and NSFC Key Program (No. 21237003).

Received: December 5, 2016
Revised: January 30, 2017
Published online:

[1] Y. Hu, Y. Zhang, C. Xu, L. Lin, R. L. Snyder, Z. L. Wang, *Nano Lett.* **2011**, *11*, 2572.
[2] G. T. Hwang, H. Park, J. H. Lee, S. Oh, K. I. Park, M. Byun, H. Park, G. Ahn, C. K. Jeong, K. No, H. Kwon, S. G. Lee, B. Joung, K. J. Lee, *Adv. Mater.* **2014**, *26*, 4880.
[3] J. H. Lee, K. Y. Lee, M. K. Gupta, T. Y. Kim, D. Y. Lee, J. Oh, C. Ryu, W. J. Yoo, C. Y. Kang, S. J. Yoon, J. B. Yoo, S. W. Kim, *Adv. Mater.* **2014**, *26*, 765.
[4] F. R. Fan, Z. Q. Tian, Z. L. Wang, *Nano Energy* **2012**, *1*, 328.
[5] X. Chen, M. Iwamoto, Z. Shi, L. Zhang, Z. L. Wang, *Adv. Funct. Mater.* **2015**, *25*, 739.
[6] G. Zhu, J. Chen, T. Zhang, Q. Jing, Z. L. Wang, *Nat. Commun.* **2014**, *5*, 3426.
[7] K. Y. Lee, J. Chun, J. Lee, K. N. Kim, N. R. Kang, J. Y. Kim, M. H. Kim, K.-S. Shin, M. K. Gupta, J. M. Baik, S.-W. Kim, *Adv. Mater.* **2014**, *26*, 5037.
[8] J. W. Zhong, Y. Zhang, Q. Z. Zhong, Q. Y. Hu, B. Hu, Z. L. Wang, J. Zhou, *ACS Nano* **2014**, *8*, 6273.
[9] K. Y. Lee, M. K. Gupta, S.-W. Kim, *Nano Energy* **2015**, *14*, 139.
[10] Z. L. Wang, J. Chen, L. Lin, *Energy Environ. Sci.* **2015**, *8*, 2250.
[11] X. Chen, T. Jiang, Y. Yao, L. Xu, Z. Zhao, Z. L. Wang, *Adv. Funct. Mater.* **2016**, *26*, 4906.
[12] X. Chen, X. Pu, T. Jiang, A. Yu, L. Xu, Z. L. Wang, *Adv. Funct. Mater.* **2017**, *27*, 1603788.
[13] H. Conrad, H. Schenk, B. t. Kaiser, S. Langa, M. Gaudet, K. Schimmanz, M. Stolz, M. Lenz, *Nat. Commun.* **2015**, *6*, 10078.
[14] W.-M. Zhang, H. Yan, Z.-K. Peng, G. Meng, *Sens. Actuators* **2014**, *A 214*, 187.
[15] K. Umeda, K. Kobayashi, K. Matsushige, H. Yamada, *AIP* **2012**, *101*, 123112.
[16] F. Carpi, S. Bauer, D. D. Rossi, *Mater. Sci.* **2010**, *330*, 1759.
[17] D. R. Link, E. Grasland-Mongrain, A. Duri, F. Sarrazin, Z. Cheng, G. Cristobal, M. Marquez, D. A. Weitz, *Angew. Chem. Int. Ed.* **2006**, *45*, 2556.
[18] C. K. Jeong, K. M. Baek, S. Niu, T. W. Nam, Y. H. Hur, D. Y. Park, G.-T. Hwang, M. Byun, Z. L. Wang, Y. S. Jung, K. J. Lee, *Nano Lett.* **2014**, *14*, 7031.
[19] L. Zheng, Z.-H. Lin, G. Cheng, W. Wu, X. Wen, S. Lee, Z. L. Wang, *Nano Energy* **2014**, *9*, 291.
[20] D. Choi, H. Lee, D. J. Im, I. S. Kang, G. Lim, D. S. Kim, K. H. Kang, *Sci. Rep.* **2013**, *3*, 2037.
[21] L. Zheng, G. Cheng, J. Chen, L. Lin, J. Wang, Y. S. Liu, H. X. Li, Z. L. Wang, *Adv. Energy Mater.* **2015**, *5*, 1501152.
[22] S. Wang, Y. Xie, S. Niu, L. Lin, C. Liu, Y. S. Zhou, Z. L. Wang, *Adv. Mater.* **2014**, *26*, 6720.
[23] Y. Sun, X. Huang, S. Soh, *Angew. Chem.* **2016**, *128*, 1.
[24] D. Choi, S. Lee, S. M. Park, H. Cho, W. Hwang, D. S. Kim, *Nano Res.* **2015**, *8*, 2481.
[25] Z. H. Lin, G. Cheng, S. M. Lee, K. C. Pradel, Z. L. Wang, *Adv. Mater.* **2014**, *26*, 4690.
[26] M. Miwa, A. Nakajima, A. Fujishima, K. Hashimoto, T. Watanabe, *Langmuir* **2000**, *16*, 5754.
[27] Z. Yoshimitsu, A. Nakajima, T. Watanabe, K. Hashimoto, *Langmuir* **2002**, *18*, 5818.